

HOW FAR ARE THE SOURCES OF ICECUBE NEUTRINOS? CONSTRAINTS FROM THE DIFFUSE TEV GAMMA-RAY BACKGROUND

XIAO-CHUAN CHANG^{1,2}, RUO-YU LIU^{1,3}, XIANG-YU WANG^{1,2}¹ School of Astronomy and Space Science, Nanjing University, Nanjing, 210093, China; xywang@nju.edu.cn² Key laboratory of Modern Astronomy and Astrophysics (Nanjing University), Ministry of Education, Nanjing 210093, China³ Max-Planck-Institut für Kernphysik, 69117 Heidelberg, Germany*Draft version March 31, 2019*

ABSTRACT

The nearly isotropic distribution of the TeV-PeV neutrinos recently detected by IceCube suggests that they come from sources at distance beyond our Galaxy, but how far they are is unknown due to lack of any associations with known sources. In this paper, we propose that the cumulative TeV gamma-ray emission accompanying with the neutrinos can be used to constrain the distance of these neutrinos, since the opacity of TeV gamma rays due to absorption by the extragalactic background light (EBL) depends on the distance that TeV gamma rays have travelled. As the diffuse extragalactic TeV background measured by *Fermi* is much weaker than the expected cumulative flux associated with IceCube neutrinos, the majority of IceCube neutrinos, if their sources are transparent to TeV gamma rays, must come from distances larger than the horizon of TeV gamma rays. We find that above 80% of the IceCube neutrinos should come from distances at redshift $z > 0.5$. Thus, any search for nearby sources correlated with IceCube neutrinos would normally yield negative result. We also find that, to explain the flux of neutrinos under the TeV emission constraint, the evolution of neutrino source density with redshift must be at least as fast as the the cosmic star-formation rate.

Subject headings: neutrinos—cosmic rays

1. INTRODUCTION

The IceCube Collaboration recently announced the discovery of extraterrestrial neutrinos (Aartsen et al. 2013, 2014a, 2015a). The sky distribution of these events is consistent with isotropy (Aartsen et al. 2014a). Such an isotropic distribution could be produced as long as the distance of the source is significantly larger than the size of the Galactic plane, thus extragalactic astrophysical objects are usually proposed as their sources, but a Galactic halo origin is also possible (Taylor et al. 2014). The proposed extragalactic sources include galaxies with intense star-formation (Loeb & Waxman 2006; He et al. 2013; Murase et al. 2013; Liu et al. 2014; Chang & Wang 2014; Tamborra et al. 2014; Chang et al. 2015; Chakraborty & Izquierre 2015; Senno et al. 2015a; Bartos & Marka 2015), jets and/or cores of active galactic nuclei (AGNs) (Stecker et al. 1991; Kalashev et al. 2014; Kimura et al. 2015; Padovani & Resconi 2014), gamma-ray bursts (Waxman & Bahcall 1997; He et al. 2012; Liu & Wang 2013; Murase & Ioka 2013; Bustamante et al. 2015; Fraija 2015) and etc. The large uncertainty in our current knowledge about the distance of neutrinos is due to that so far no associated astrophysical sources have been identified.

A common way to produce astrophysical high-energy neutrinos is the decay of charged pions created in inelastic hadronuclear (pp) and/or photohadronic ($p\gamma$) processes of cosmic rays (CRs), in which high-energy gamma rays will be also generated from the decay of synchronously created neutral pions. The emissivity of gamma rays and neutrinos are related through $E_\gamma Q_\gamma(E_\gamma) \approx (2/3) E_\nu Q_\nu(E_\nu)|_{E_\nu=E_\gamma/2}$ (for pp process), where Q represents the emission rate per source. VHE gamma rays ($\gg 100$ GeV), unlike neutrinos which propagate through the universe almost freely, will be significantly absorbed by the extragalactic background light (EBL) and cosmic microwave background (CMB) during the propaga-

tion through intergalactic space if the source distance is larger than the mean free path of these gamma rays. For a TeV photon, the optical depth would be larger than unity beyond $z \sim 0.1$. Therefore, the cumulative flux of VHE gamma rays which associate with the neutrinos carries the information about the distance of neutrino sources. Significant progresses have been made in our understanding of the extragalactic gamma-ray background (EGB) in recent years. The spectrum of the EGB has now been measured with the Fermi-LAT in the energy range from 0.1 to 820 GeV (Ackermann et al. 2015a). New studies of the blazar source count distribution at gamma-ray energies above 50 GeV place an upper limit on the residual non-blazar component of the EGB (Ackermann et al. 2015b). In this paper, we use this upper limit at TeV energy to constrain the distance and the evolution of the bulk population of neutrino sources. The distance information has important implications for the search of correlations between observed neutrino events and nearby gamma-ray sources. If the inferred distance of the majority of neutrinos is large, the search for nearby correlated sources would undoubtedly yield negative result. It may also explain the negative result of search for the correlation between neutrinos and ultra-high energy cosmic rays (Aartsen et al. 2015b), which originate within $\lesssim 100$ Mpc.

In §2, we first present how we use the TeV emission to place constraints. Then, in §3, we give the input conditions and assumptions. We give our results in §4. Finally, we give the conclusions and discussions in §5.

2. THE METHOD FOR CONSTRAINTS

In the astrophysical origin scenario, neutrinos (also gamma rays) are produced in various discrete astrophysical objects, so the total observed neutrino flux comes from the sum of contributions of each individual source, rather than from truly diffuse emissions. We assume that the neutrino sources are transparent to gamma rays, and only consider the attenuation

in the intergalactic space due to EBL and CMB absorption. It is reasonable to assume that the sources follow a poisson distribution, then the probability density that the n th-closest source locates at a comoving distance r can be expressed as

$$p(n, r) = \frac{4\pi N^{n-1}}{(n-1)!} e^{-N} r^2 \rho \quad (1)$$

where N is the expectation number of the sources within a spherical comoving volume V with radius r , i.e. $N = \int \rho 4\pi r^2 dr$. The source number density ρ can be expressed as $\rho = \rho(0)f(z)$, where $f(z)$ represents the evolution of the source density with redshift. So the expected comoving distance where the n th-closest source locates is $\bar{r}(n) = \int_0^\infty p(n, r) r dr$.

The influence of source number density on the gamma ray background is complicated. If the spatial number density of the sources is low, given a measured diffuse neutrino flux, the corresponding pionic gamma ray luminosity of each source should be relatively high, so this kind of sources are easier to be resolved by instruments. By contrast, if the spatial number density of the source is high, the luminosity should be smaller. As a result, these sources are more likely to be unresolved and hence the emitted gamma rays contribute to the isotropic diffuse gamma-ray background (IGRB). If more nearby sources are resolved from background, the distant sources are allowed to be brighter without violating the IGRB data. Such a requirement can be expressed as,

$$\Phi_{\gamma,un}(E_\gamma) = \sum_{F_n < F_{sens}}^n F_n(E_\gamma) \leq \Phi_{IGRB}(E_\gamma). \quad (2)$$

where $\Phi_{\gamma,un}(E_\gamma)$ represents the cumulative flux of unresolved sources, $F_n(E_\gamma)$ represents the flux of the n -th closest source and F_{sens} is the point source sensitivity of *Fermi*-LAT.

In the same time, the resolved sources contribute to EGB together with the unresolved ones, so they satisfy

$$\Phi_{\gamma,tot}(E_\gamma) = \sum F_n(E_\gamma) \leq \Phi_{EGB}(E_\gamma). \quad (3)$$

where $\Phi_{\gamma,tot}(E_\gamma)$ represents the cumulative flux of all sources, including both resolved and unresolved ones. In our calculation, we use the broadband sensitivity provided by *Fermi*-LAT performance in Pass 8¹. Assuming the gamma-ray spectral index $\gamma = 2$, the sensitivity reaches the level of $F_{sens} \sim 2 \times 10^{-13}$ ergs cm $^{-2}$ s $^{-1}$. According to this, we could determine whether a point source could be resolved or not. Based on the above two requirements (Eqs. 2 and 3), we will see that the maximum neutrino flux is constrained by *Fermi* data.

For simplicity, we assume all the sources have the same intrinsic gamma-ray luminosity L' which relates to the gamma-ray spectral emissivity of each source $Q'_\gamma(E'_\gamma)$ by $L' = \int_{E'_{min}}^{E'_{max}} Q'_\gamma(E'_\gamma) dE'_\gamma$, with E'_{max} and E'_{min} being the maximum and minimum energy of emitted photon. Here the prime denotes quantities measured in the rest frame of the source (i.e., $E'_\gamma = E_\gamma(1+z)$). While low-energy gamma rays can propagate to us from the sources freely, VHE gamma rays may be

absorbed by the EBL and CMB photons in the intergalactic space. The produced electron/positron pairs will also interact with EBL and CMB photons and generate secondary gamma rays by inverse-Compton scattering. Such a cycle is called cascade, and it will continue until the new generated photons are not energetic enough to produce electron/positron pairs by interacting with the background photons. As a result, the absorbed high-energy gamma rays are reprocessed to a bunch of lower-energy ones. So the total gamma ray flux after propagation consists of a primary component which is the unabsorbed gamma rays and a cascade component, i.e.,

$$F(E_\gamma) = \left\{ Q'_\gamma [(1+z)E_\gamma] e^{-\tau(E_\gamma)} + Q_{\gamma,cas}(E_\gamma) \right\} / 4\pi \bar{r}^2, \quad (4)$$

where $\tau(E_\gamma)$ is the optical depth for a photon of energy E_γ . In this paper, we use the optical depth provided by Finke et al. (2010)² and discuss the effect of other EBL models.

Since the results depend on the density of the neutrino source, we will consider three different cases:

- 1) a high-density source case, such as star-forming/starburst galaxies. The density of starburst galaxy is about 4×10^{-4} Mpc $^{-3}$. Starburst galaxies, due to their high star formation rates, and hence large number of supernova or hypernova remnants therein, are huge reservoirs of cosmic ray (CR) protons with energy up to EeV (Wang et al. 2007). These CRs produce high-energy neutrinos by colliding with gases in galaxies (Loeb & Waxman 2006; Liu et al. 2014);
- 2) a middle-density case, such as clusters of galaxies. The density of clusters of galaxies is about $10^{-5} \sim 10^{-6}$ Mpc $^{-3}$ depending on the mass selection (Jenkins et al. 2001). Here we choose 4×10^{-6} Mpc $^{-3}$ as a reference value. Galaxy clusters, which have been argued to be able to accelerate CRs and considered as possible sources for high-energy neutrinos (Murase et al. 2008).
- 3) a low-density case, such as blazars. The density of blazars is ranging from 10^{-9} to several 10^{-8} Mpc $^{-3}$ (Ajello et al. 2012, 2014). We choose 4×10^{-8} Mpc $^{-3}$ as a reference value. As blazars are powerful gamma-ray sources, there have been extensive discussions about their possibility of being high-energy neutrino sources (see Ahlers & Halzen (2015) for a review).

3. ASSUMPTION ABOUT THE EXTRAGALACTIC NEUTRINO FLUX AND INJECTION SPECTRA OF GAMMA RAYS

The latest combined maximum-likelihood analysis of IceCube neutrinos gives a best-fit power law spectrum with a spectral index of $\gamma = 2.50 \pm 0.09$ in the energy range between 25 TeV and 2.8 PeV, and an all-flavor flux of $\phi = (6.7^{+1.1}_{-1.2}) \cdot 10^{-18}$ GeV $^{-1}$ s $^{-1}$ sr $^{-1}$ cm $^{-2}$ at 100 TeV (Aartsen et al. 2015a). Interestingly, The IceCube collaboration have tested the hypothesis of isotropy by analyzing data in the northern and southern sky respectively. Compared to the all-sky result, the spectrum of the events in the northern sky can be better fitted by a harder power-law ($\gamma = 2.0^{+0.3}_{-0.4}$), while the southern one favors a slightly softer spectrum ($\gamma = 2.56 \pm 0.12$). However, the result is not conclusive, as the discrepancy could be simply caused by a statistical fluctuation. Alternatively, it could be due to an additional component that is present in only one of the hemispheres (either an unmodeled background component, or e.g. a component from the inner Galaxy).

As indicated in some recent studies (Ackermann et al. 2015b), the EGB is dominated by blazars above 50 GeV at

¹ http://www.slac.stanford.edu/exp/glast/groups/canda/lat_Performance.htm

² <http://www.phy.ohio.edu/~finke/EBL/index.html>

the level of $86^{+16}_{-14}\%$. If it is correct, this implies a strong suppression of contributions from other sources with a flux of $\lesssim 2-3 \times 10^{-8} \text{ GeV cm}^{-2} \text{ s}^{-1} \text{ sr}^{-1}$ at 50 GeV. If the neutrino sources are transparent to gamma rays, the neutrino flux per-flavor is constrained to be at most $\sim 10^{-8} \text{ GeV cm}^{-2} \text{ s}^{-1} \text{ sr}^{-1}$, which is much lower than the measured flux at 25 TeV. To solve this tension, it has been proposed that TeV neutrinos may come from some hidden sources, i.e. they are not transparent to gamma rays (Murase et al. 2015; Bechtol et al. 2015). The transparent sources can only explain the PeV neutrino flux ($\sim 10^{-8} \text{ GeV cm}^{-2} \text{ s}^{-1} \text{ sr}^{-1}$) without exceeding the non-blazar EGB component.

Consider the above uncertainties, we divide our discussions into two cases. In the first case, we assume that the gamma-ray background is only relevant to $\gtrsim 100$ TeV neutrinos whose sources are transparent to gamma-rays and ~ 25 TeV neutrinos may originate from hidden sources (Murase et al. 2015; Tamborra & Ando 2015; Senno et al. 2015b; Wang & Liu 2015) or from a component of the inner Galaxy. We adopt the non-blazar EGB as obtained by Ackermann et al. (2015b) to place constraints. The gamma-ray spectrum at the source should follow the spectrum of neutrinos, which is assumed to be a flat spectrum with index $\gamma = 2.0$ below 1 PeV, as predicted by the Fermi acceleration mechanism, and a steeper spectrum with $\gamma = 2.5$ above 1 PeV (Aartsen et al. 2014a). In the second case, we assume that extragalactic neutrinos has a flux as high as $10^{-7} \text{ GeV cm}^{-2} \text{ s}^{-1} \text{ sr}^{-1}$ and their sources are transparent to gamma rays. Since the associated gamma rays with TeV neutrino significantly exceeds the non-blazar EGB, we relax this requirement by considering the full EGB given in Ackermann et al. (2015a), allowing blazars to contribute to IceCube neutrinos. In this case, the neutrino spectrum at the source is assumed to follow a broken power law with the spectral index $\gamma = 2$ at $E_\nu < 25$ TeV and $\gamma = 2.5$ at $E_\nu > 25$ TeV (Aartsen et al. 2015a).

In short, we assume two kinds of injection spectrum of gamma rays, i.e.,

$$\text{Case}(a) : \begin{cases} n(E_\gamma) \propto E_\gamma^{-2}, & E_\gamma < 2(1+z)\text{PeV} \\ n(E_\gamma) \propto E_\gamma^{-2.5}, & E_\gamma \geq 2(1+z)\text{PeV}, \end{cases} \quad (5)$$

and

$$\text{Case}(b) : \begin{cases} n(E_\gamma) \propto E_\gamma^{-2}, & E_\gamma < 50(1+z)\text{TeV} \\ n(E_\gamma) \propto E_\gamma^{-2.5}, & E_\gamma \geq 50(1+z)\text{TeV}. \end{cases} \quad (6)$$

4. RESULTS

When the cumulative TeV flux is fixed, as constrained by the IGRB and EGB data, the total neutrino flux is affected by two factors. First, as we already mentioned above, the spatial density of the sources is an important effect. If the density is smaller, the luminosity of individual source is larger and hence more nearby sources will be resolved. Gamma rays from these resolved sources will not be counted into IGRB while they still contribute to diffuse neutrino flux. The second factor is the distance of the source or the evolution of the source density with redshift. TeV photons from more distant sources will be more likely to be absorbed during propagation to the earth, while neutrinos will not. So the neutrino flux will be higher if the fraction of distant sources is higher (or the density evolution with redshift is stronger).

4.1. Case (a)

In this case, we assume that EGB and IGRB are only relevant to $\gtrsim 100$ TeV neutrinos and adopt the non-blazar EGB obtained by Ackermann et al. (2015b) as an upper limit of the cumulative flux from neutrino sources. First, we want to know how large fraction nearby sources can contribute to the observed neutrino flux. In Fig. 1, we fix the limit of gamma-ray flux to be $2.5 \times 10^{-9} \text{ GeV cm}^{-2} \text{ s}^{-1} \text{ sr}^{-1}$ at 820 GeV, which corresponds to 14% of the total EGB (i.e., the non-blazar EGB³), and calculate the maximally allowed neutrino flux at PeV as a function of the boundary distance z_{\max} . The boundary distance z_{\max} means that all the sources contributing to IGRB/EGB locate within the redshift z_{\max} . The spectra of gamma rays and neutrinos are assumed to follow Eq. (5).

The left panel of Fig. 1 shows the maximum neutrino flux at 1 PeV without violating the non-blazar EGB. The figure indicates that, in the middle and high source density cases, only a small fraction of neutrinos come from low redshift sources. The sources below $z_{\max} = 0.5$ can account for at most a fraction of 20% of the total neutrino flux. Thus, the majority of neutrinos observed by IceCube should come from distance further than $z_{\max} = 0.5$. We can also see that the redshift evolution of the sources should not be slower than that of cosmic star-formation rate (SFR) to account for the observed neutrino flux. By contrast, a constant evolution of sources (i.e. $f(z) = \text{const}$) seems to be able to explain all the neutrino flux in the low density case. However, in this case, the nearest point sources should have been detected by IceCube, given its sensitivity of $E^2 dE/dN \sim 10^{-9} \text{ GeV s}^{-1} \text{ cm}^{-2}$ (Aartsen et al. 2014b). This suggests that the source density should not be too low unless that the majority of gamma rays do not come from the same hadronic process that produce neutrinos. We then consider the latter possibility, and find that the IceCube non-detection of the nearest point sources requires that the ratio between the emissivity of neutrinos and that of gamma rays should be $\lesssim 8\%$. We then recalculate the maximum neutrino flux with the new ratio, which is shown in the right panel of Fig. 1. We find that, under this extra constraint, the source density evolution can not be slower than cosmic SFR in the low-density case.

The requirement of a fast evolution of the source density with redshift can also be seen by comparing the expected cumulative TeV emission accompanying the production of neutrinos with the observed gamma-ray background data. Fig. 2 shows the cumulative gamma-ray emission for different redshift evolution scenarios. Here we adopt the high source density case for illustration, while the result holds for other source density cases. We can see that only when the evolution is not slower than that of the cosmic SFR, the cumulative TeV flux is consistent with the non-blazar EGB limit. In all three density evolution scenarios, however, the flux at 10-100 GeV are quite similar, which is naturally expected since 10-100 GeV gamma rays are almost as transparent as neutrinos. This demonstrates the unique role of TeV flux in constraining the evolution of neutrino source density.

4.2. Case (b)

In this case, we consider ~ 25 TeV neutrinos also originate from extragalactic sources that are transparent to gamma rays. Since the co-produced gamma ray flux would then be much higher than the non-blazar EGB limit, we relax the con-

³ Ackermann et al. (2015b) find that blazars constitute about 86% of the integrated photon flux above 50 GeV. We here assume the spectrum of the summed emission of all blazars are identical to that of the observed EGB.

straint by the non-blazar EGB and use the full EGB as an upper limit (Ackermann et al. 2015a). The IGRB constraint becomes important for this case and we also consider this constraint. So, we fix the upper limit of the cumulative gamma-ray flux at 820 GeV to be $6 \times 10^{-9} \text{ GeV cm}^{-2} \text{ s}^{-1} \text{ sr}^{-1}$ (IGRB) for unresolved sources and $3 \times 10^{-8} \text{ GeV cm}^{-2} \text{ s}^{-1} \text{ sr}^{-1}$ (EGB) for all the sources. Fig. 3 shows the maximum neutrino flux at 100 TeV as a function of the boundary redshift z_{\max} , by assuming a gamma-ray spectrum of Eq. (6). The results imply a similar preference for the source distribution at high redshift. In the high and middle density cases, the source density evolution should not be slower than cosmic SFR evolution. For the low density case, the situation is also similar. When considering the neutrino non-detection constraint, the ratio between the emissivity of neutrinos and that of gamma-rays should be $\lesssim 15\%$. Then we find that a fast evolution is also needed for the low-density case, as shown in the right panel of Fig. 3.

Like Case (a), we compare the cumulative gamma-ray emission of unresolved sources with the IGRB data in Fig. 4 for the high source density case. We find that, in order not to exceed the IGRB, the source density must evolve faster than SFR.

The calculation in Case (b) used the full EGB data given in Ackermann et al. (2015a). Latest studies of the EGB composition at energies above 50 GeV find a dominant contribution by blazars including the dim ones below the current detection limit of *Fermi*. If this new analysis is correct and the neutrino sources are transparent to gamma-rays, blazars, dominated in number by low-luminosity ones, have to be the leading sources of TeV neutrinos. Our finding of a fast density evolution for the neutrino sources then applies to these low-luminosity blazars.

5. DISCUSSIONS AND CONCLUSIONS

In the above calculation, we used the EBL model given by Finke et al. (2010). Different EBL models might affect the opacity of TeV gamma rays and we thus study this effect. We use the upper and lower bounds on the opacity given by Stecker (2013) as the boundary of EBL uncertainties. Fig. 5 shows the influence on cumulative gamma-ray emission when varying the EBL opacity within this boundary. For illustration, we consider the Case (b) and use a density of $4 \times 10^{-4} \text{ Mpc}^{-3}$ and SFR evolution. We find that, even for the strongest EBL intensity model, the cumulative TeV flux decreases only slightly (less than 20%) compared to the case using the EBL model given by Finke et al. (2010). Thus, we conclude that EBL model uncertainty does not change our conclusion that a fast density evolution is required.

In previous sections, we obtained the constraint on the source density evolution assuming that the gamma-ray (or neutrino) luminosity is the same for all sources. If the gamma-ray/neutrino luminosity of the source also varies with redshift, it is then the gamma-ray/neutrino emission rate density, rather than source number density, that plays the role. The emission rate density can be expressed as $g(z)\rho(z)$, where $\rho(z)$ represents the source number density and $g(z)$ is the factor accounting for the luminosity evolution of the source. As long as their product ($g(z)\rho(z)$), has a fast evolution with redshift, the requirement is fulfilled. So the source number density may not need to evolve that fast if the factor $g(z)$ evolves fast enough. The factor $g(z)$ could originate from various physical causes. For example, in the starburst galaxy scenario for IceCube neutrinos, cosmic rays may have a higher efficiency converting their energies to pions in higher-redshift galaxy

due to a higher gas density therein, which leads to a large $g(z)$ at high redshift (Chang et al. 2015).

To summarize, we find that extragalactic TeV background is a useful tool to study the distance and density evolution of neutrino sources. We have considered two versions of IGRB/EGB scenarios and used different injection spectra correspondingly. In both cases, we find that only a small fraction of neutrinos are allowed to come from low-redshift sources in order not to exceed the diffuse TeV background limit. To account for the IceCube neutrino flux, the density of neutrino sources must have a fast evolution with redshift. Interestingly, this is consistent with the independent result obtained by the tomographic constraints (Ando et al. 2015). As our result shows that the IceCube neutrinos come dominantly from distant sources at high redshift, any models arguing for nearby sources can be ruled out. Also, any search for nearby sources correlated with IceCube neutrinos would undoubtedly yield negative result. Instead, we suggest to search for correlations with potential cosmic ray accelerators at high redshifts.

REFERENCES

Aartsen, M. G., Abbasi, R., Abdou, Y., et al. 2013, Physical Review Letters, 111, 021103
 Aartsen, M. G., Ackermann, M., Adams, J., et al. 2014a, Physical Review Letters, 113, 101101
 Aartsen, M. G.; Ackermann, M.; Adams, J.; et al. 2014b, ApJ, 796, 109
 Aartsen, M. G., Abraham, K., Ackermann, M., et al. 2015a, ApJ, 809, 98
 Aartsen, M. G., Abraham, K., et al. 2015b, arXiv:1511.09408
 Ackermann, M., Ajello, M., Albert, A., et al. 2015, ApJ, 799, 86
 Ackermann et al. 2015b, arXiv:1511.00693
 Ahlers, M., & Halzen, F. 2014, Phys. Rev. D, 90, 043005
 Ahlers, M., & Halzen, F. 2015, Reports on Progress in Physics, 78, 126901
 Ajello, M., Shaw, M. S., Romani, R. W., et al. 2012, ApJ, 751, 108
 Ajello, M., Romani, R. W., Gasparini, D., et al. 2014, ApJ, 780, 73
 Ando, S., Tamborra, I., & Zandanel, F. 2015, Physical Review Letters, 115, 221101
 Bartos, I., & Marka, S. 2015, arXiv:1509.00983
 Bechtol, K., Ahlers, M., Di Mauro, M., Ajello, M., & Vandenbroucke, J. 2015, arXiv:1511.00688
 Bustamante, M.; Baerwald, P.; Murase, K.; Winter, W. 2015, Nature Communications, 6, 6783
 Chakraborty, S., & Izaguirre, I. 2015, Physics Letters B, 745, 35
 Chang, X.-C., & Wang, X.-Y. 2014, ApJ, 793, 131
 Chang, X.-C., Liu, R.-Y., & Wang, X.-Y. 2015, ApJ, 805, 95
 Finke, J. D., Razzaque, S., & Dermer, C. D. 2010, ApJ, 712, 238
 Fraija, N. 2015, arXiv:1508.03009
 He, H. N.; Liu, R. Y., Wang, X. Y., Nagataki, S., Murase, K. & Dai, Z. G., 2012, ApJ, 752, 29
 He, H.-N.; Wang, T.; Fan, Y.-Z.; Liu, S.-M.; Wei, D.-M., Phys. Rev. D, 87, 063011
 Jenkins, A., Frenk, C. S., White, S. D. M., et al. 2001, MNRAS, 321, 372
 Kalashev, O., Semikoz, D., & Tkachev, I. 2014, arXiv:1410.8124
 Kimura, S. S., Murase, K., & Toma, K. 2015, ApJ, 806, 159
 Liu, R.-Y., Wang, X.-Y., 2013, ApJ, 766, 73
 Liu, R.-Y., Wang, X.-Y., Inoue, S., Crocker, R., & Aharonian, F. 2014, Phys. Rev. D, 89, 083004
 Loeb, A., & Waxman, E. 2006, JCAP, 5, 3
 Murase, K., Inoue, S., & Nagataki, S. 2008, ApJ, 689, L105
 Murase, K., Ahlers, M., & Lacki, B. C. 2013, Phys. Rev. D, 88, 121301
 Murase, K., & Ioka, K. 2013, Physical Review Letters, 111, 121102
 Murase, K., Guetta, D., & Ahlers, M. 2015, arXiv:1509.00805
 Padovani, P., & Resconi, E. 2014, MNRAS, 443, 474
 Senno, N., Mészáros, P., Murase, K., Baerwald, P., & Rees, M. J. 2015, ApJ, 806, 24
 Senno, N., Murase, K., & Meszaros, P. 2015, arXiv:1512.08513
 Stecker, F. W., Done, C., Salamon, M. H., & Sommers, P. 1991, Physical Review Letters, 66, 2697
 Stecker, F. W. 2013, arXiv:1302.2065
 Tamborra, I., Ando, S., & Murase, K. 2014, JCAP, 9, 043
 Tamborra, I., & Ando, S. 2015, arXiv:1512.01559
 Taylor, A. M., Gabici, S., & Aharonian, F. 2014, Phys. Rev. D, 89, 103003

Wang, X.-Y., Razzaque, S., Mészáros, P., & Dai, Z.-G. 2007, Phys. Rev. D, 76, 083009

Wang, X.-Y., & Liu, R.-Y. 2015, arXiv:1512.08596

Waxman, E., & Bahcall, J. 1997, Physical Review Letters, 78, 2292

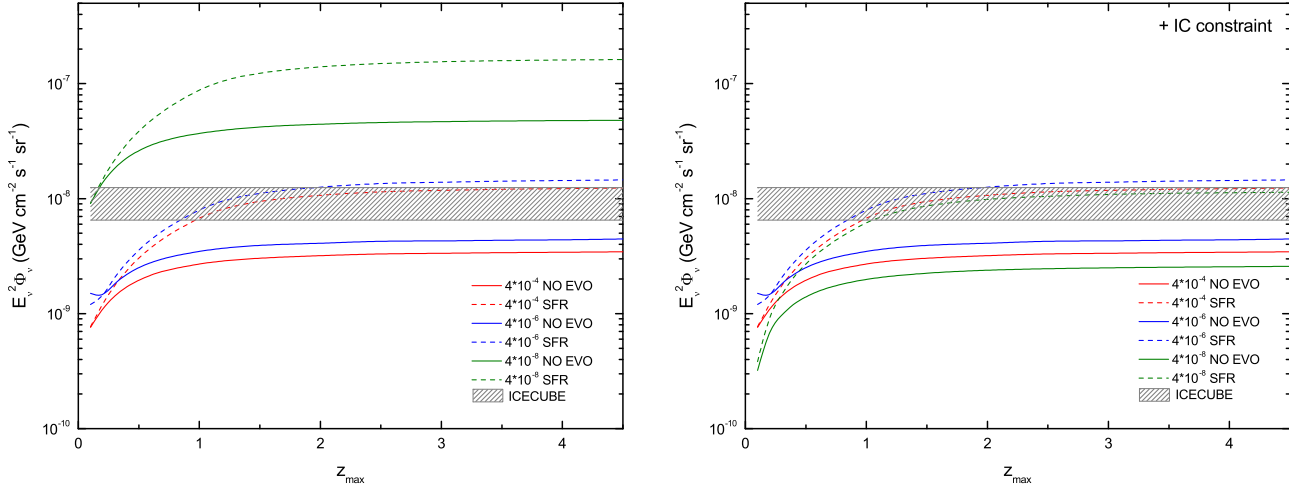


Figure 1. The maximally-allowed neutrino flux at 1PeV under the constraint of the non-blazar TeV background as a function of the boundary redshift z_{\max} in Case (a). The red, blue and green lines represent the cases with source density of $4 \times 10^{-4} \text{ Mpc}^{-3}$, $4 \times 10^{-6} \text{ Mpc}^{-3}$ and $4 \times 10^{-8} \text{ Mpc}^{-3}$, respectively. The solid and dashed lines represent, respectively, no evolution and SFR evolution of the source density with redshift. The grey shaded area represents the observed neutrino flux (per flavor) by IceCube at 1PeV with errors (Aartsen et al. 2014a). In the right panel, an extra constraint due to the IceCube non-detection of nearest point sources is considered.

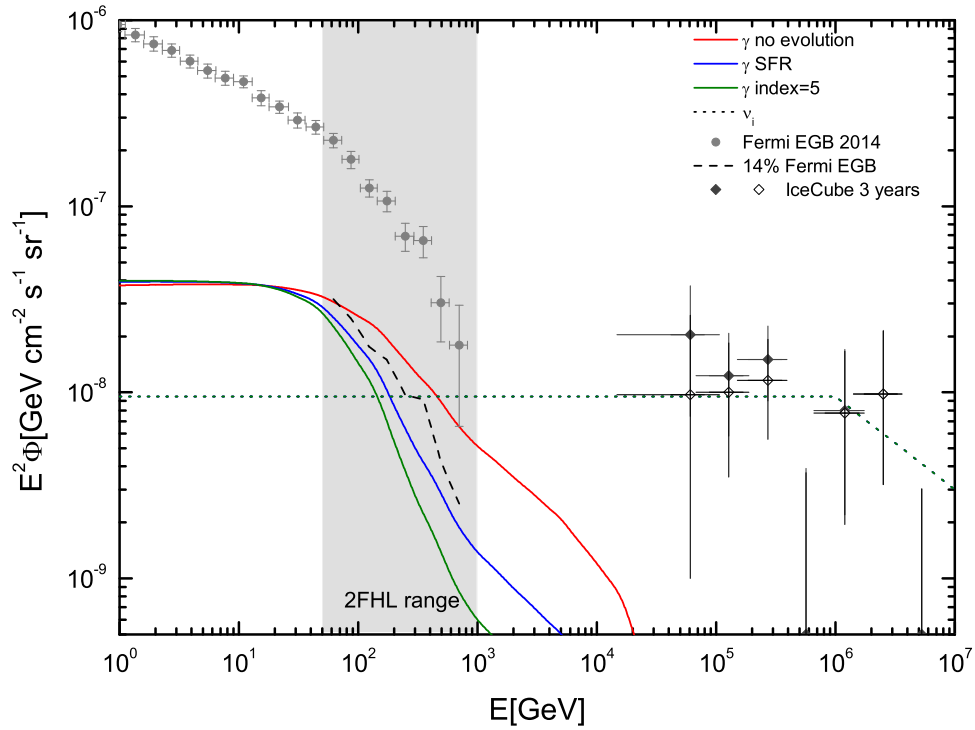


Figure 2. The cumulative gamma-ray emission associated with production of IceCube neutrinos in Case (a) for different redshift evolution models. The spectrum of the neutrinos used in the calculation is shown by the short dashed line. The red, blue and green lines show, respectively, the case assuming no redshift evolution, SFR evolution and an evolution given by $\propto (1+z)^5$ at $z < 1$ and $\propto (1+z)^0$ at $z > 1$. The IGRB data from *Fermi*-LAT (Ackermann et al. 2015a) are denoted by grey dots and the thick dashed line shows 14% of EGB for no-blazars sources (Ackermann et al. 2015b). The IceCube data are denoted by black dots (Aartsen et al. 2014a). In the calculation, we use the case of source density of $4 \times 10^{-4} \text{ Mpc}^{-3}$.

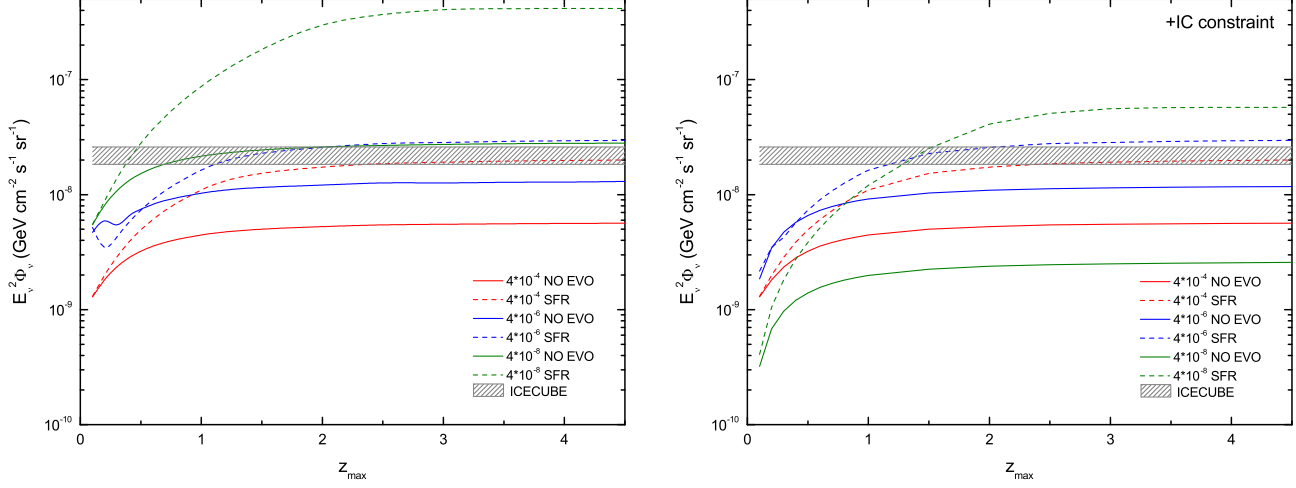


Figure 3. Same as Figure 1, but for Case (b). Note that all the neutrino fluxes here correspond to the value at the reference energy of 100 TeV. The horizontal shaded region corresponds to the observed flux at 100 TeV in the combined analysis (Aartsen et al. 2015a).

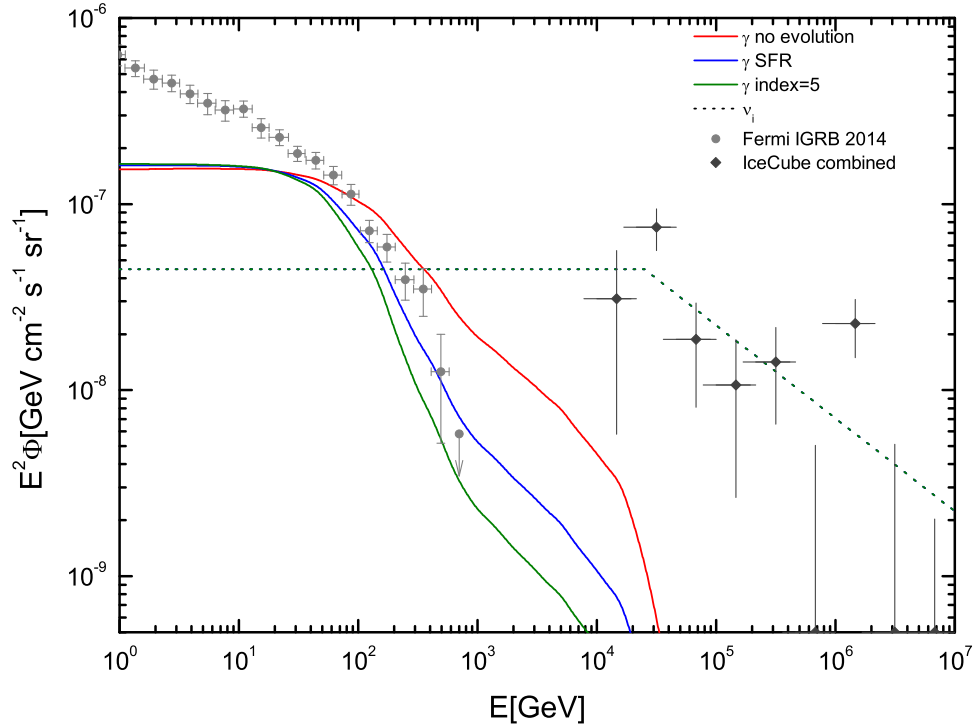


Figure 4. Comparison between the cumulative gamma-ray emission of unresolved sources and the IGRB data for different density evolution models. In the calculation, we use the case of source density of $4 \times 10^{-4} \text{ Mpc}^{-3}$. The neutrino flux data used in the calculation correspond to the combined analysis of IceCube data (Aartsen et al. 2015a).

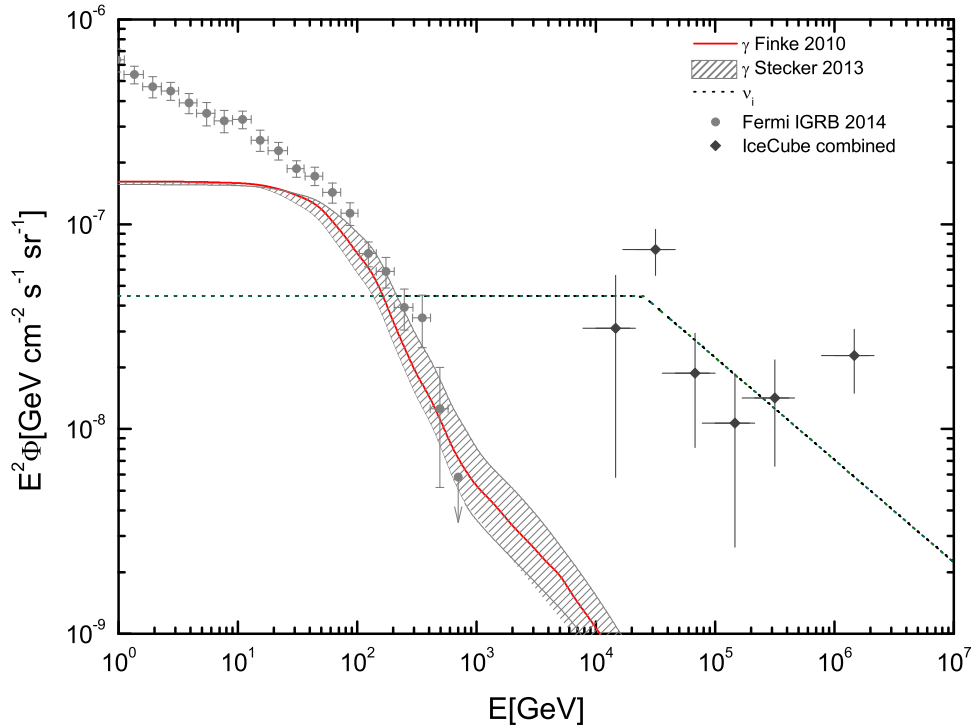


Figure 5. Same as figure 4, but considering the uncertainty in EBL models. We use the upper and lower bounds on the opacity given by Stecker (2013) as the boundary of EBL uncertainties. The red line shows the gamma-ray emission corresponding to the EBL model provided by Finke et al. (2010). In the calculation, we use a source density of $4 \times 10^{-4} \text{Mpc}^{-3}$ and assume SFR redshift evolution.